Impact of peroxiredoxin 3 deficiency in vascular smooth muscle cells and predictive role of impaired vascular mechanics on angiotensin-II-induced abdominal aortic aneurysm formation in mice model

Choongki Kim

Department of Medicine

The Graduate School, Yonsei University

Impact of peroxiredoxin 3 deficiency in vascular smooth muscle cells and predictive role of impaired vascular mechanics on angiotensin-II-induced abdominal aortic aneurysm formation in mice model

Choongki Kim

Department of Medicine

The Graduate School, Yonsei University

Impact of peroxiredoxin 3 deficiency in vascular smooth muscle cells and predictive role of impaired vascular mechanics on angiotensin-II-induced abdominal aortic aneurysm formation in mice model

Directed by Professor Yangsoo Jang

The Doctoral Dissertation
submitted to the Department of Medicine
the Graduate School of Yonsei University
in partial fulfillment of the requirements for the degree of
Doctor of Philosophy

Choongki Kim

December 2020

This certifies that the Doctoral Dissertation of Choongki Kim is approved.

Thesis Supervisor : Yangsoo Jang

Thesis Committee Chair : Myeong-Ki Hong

Thesis Committee Member : Goo Taeg Oh

Thesis Committee Member : Sung Ha Park

Thesis Committee Member: Ki Taek Nam

The Graduate School
Yonsei University

December 2020

ACKNOWLEDGEMENTS

I have always thought it is definitely fortunate and grateful that I had an opportunity to be a part of medical field. As a young clinical doctor and researcher, I have almost always felt rewarding to take care of patients and to devote myself to contributing knowledge of medicine. However, I was sometimes frustrated when I realized again that the science still lights very limited part of our field, and that I understand only a little bit of them. When I felt to be standing in front of enormous obstacles, my inspiring teachers, Professor Yangsoo Jang and Myeong-Ki Hong helped me to apply myself to continuing my concentration on this field. I believe that beginning of my scientific and clinical groundwork was substantially depended on them. Their inspiration will be always vital for my future steps. I also appreciate to Professor Sung Ha Park. He has always been a model as a sincere scientist and clinician. I have been much inspired by his conduct to try to be a somewhat better in my field.

Professor Goo Taeg Oh provided exceptional ideas and environments for me to explore my doctorate themes. Although I was not well capable of doing bench experiments and researches, he kindly guided and supported me with his great staff member. Especially, I appreciate Master Da-Seul Lee, who has exchanged research ideas with me as an important partner of our experiments. I

also thank Professor Ki Taek Nam for reviewing my manuscript and sparing his valuable time to suggest valuable comments to improve my research.

Although I wish that I could contribute just a trivial thing on the medicine, I am not sure if I could. However, I am sure that I will continue my efforts to contribute even small things for the medicine and my community. Lastly, I deeply appreciate my precious wife and son, Jung-In Shin and Gyu-Min Kim for their support and care. I also promise them that I will always be their sincere guardian.

Choongki Kim

<TABLE OF CONTENTS>

LIST OF FIGURES

LIST OF TABLES

ABSTRACT

Impact of peroxiredoxin 3 deficiency in vascular smooth muscle cells and predictive role of impaired vascular mechanics on angiotensin-II-induced abdominal aortic aneurysm formation in mice model

Choongki Kim

Department of Medicine
The Graduate School, Yonsei University

(Directed by Professor Yangsoo Jang)

Abdominal aortic aneurysm (AAA) is known as a degenerative vascular disease caused by increased metalloproteinase activity, vascular inflammation, and oxidative stress in the vessel wall. Peroxiredoxins (Prdx) 3 is located in mitochondria and plays an important role in scavenging endogenous oxidative stress. In the study, 24-week-old *Prdx3*$^{flox/flox}$ *SM22-Cre* mice were generated for conditional knockout of *Prdx3* in vascular smooth muscle cells which influences vasomotor function and endothelial reactivity considered as vital factors of pathogenesis of AAA. *Prdx3*$^{flox/flox}$ mice was used as a control. AAA was induced by continuous infusion of angiotensin-II achieved by subcutaneous implantation of mini-osmotic pump. Serial ultrasound evaluation was performed to observe occurrence and progression of AAA formation and to measure changes in

vascular morphology, dimensions, and mechanical properties as well. Of 14 *Prdx3*$^{flox/flox}$ *SM22-Cre* mice and 9 control mice, AAA was induced in 5 (55%) *Prdx3*$^{flox/flox}$ *SM22-Cre* mice and 5 (36%) control mice and during the study period. Although incidence of AAA, sonography-measured vascular dimensions and mechanics did not significantly differ, there was a trend that more aggravated forms of AAA were associated with *Prdx3* deficiency. Elastin degradation and calcific burden were greater in AAA occurred in *Prdx3*$^{flox/flox}$ *SM22-Cre* mice than those in control mice. Compared with aorta without aneurysmal change, AAA was associated with impaired vascular mechanics as well as rapid increase in vascular dimension. Early changes in radial wall velocity and fractional area change of aorta was observed in mice in which AAA occurred thereafter. The model including parameters of early changes in vascular mechanics had greater predictability of impending AAA compared with the model based on vascular dimensions. Noninvasive diagnostic tools with good feasibility and reproducibility may be promising for risk stratification and predicting progression of AAA.

Key words : abdominal aortic aneurysm, oxidative stress, peroxiredoxin, vascular mechanics

Impact of peroxiredoxin 3 deficiency in vascular smooth muscle cells and predictive role of impaired vascular strain on angiotensin-II-induced abdominal aortic aneurysm formation in mice model

Choongki Kim

Department of Medicine

The Graduate School, Yonsei University

(Directed by Professor Yangsoo Jang)

I. INTRODUCTION

Aortic abdominal aneurysms (AAA) are important causes of cardiovascular morbidity and mortality.[1] AAA is believed to result from an aberrant interaction between genetic factors and the environment which aggravates the normal aging processes. The mechanisms of AAA include increased metalloproteinase activity, vascular inflammation, mechanical stress and increased reactive oxygen species (ROS) production in the vessel wall.[1] However, the effective treatment for primary or secondary prevention of AAA have not been revealed in previous human studies. It is imperative to better understand the mechanisms of this

important disease and to provide new, specific drug targets for the treatment of AAA.

Many clinical studies also demonstrated the association between AAA and increased oxidative stress in human AAA. ROS production is induced by mechanical stress to the vascular wall or by cytokines. Regulating anti-oxidative enzymes, such as superoxide dismutase, catalase, and glutathione peroxidase, scavenge ROS and, hence, protect cells against oxidative stress [2]. Role of local oxidative stress in the pathogenesis of AAA has been investigated. Local production of superoxide anion was found in human aneurysms.[3] Also, endothelial and smooth muscle cells from AAA had more oxidative DNA damage.[4] The markers of systemic oxidative stress such as malondialdehyde were shown to be increased in AAA patients.[5,6] Human AAA size was closely correlated to NADPH oxidase, a major source of superoxide anion in human and animal vasculature, which provides the role of this enzyme system in the progression and development of the disease.[7] Recently, many studies have been conducted for exploring the potential modulators of AAA progression regarding oxidative stress. Paraoxonase-1 was decreased in plasma of AAA patients, and it was shown to protect against AAA development through a decrease in oxidative stress, apoptosis and inflammatory cell accumulation.[8] The role of each subtype NADPH oxidase in the process of AAA progression have been also investigated.[9,10] Major sources of vascular ROS production include NADPH oxidases, xanthine oxidase, uncoupled nitric oxide synthase, and mitochondria. Although many previous studies have focused on the role of vascular NADPH oxidases as a major source of ROS production, mitochondria

also represent one of the most significant sources of cellular ROS generation.[11,12] Mitochondrial ROS production can reach up to 2% of the electron flow, but the regulation of mitochondrial ROS generation and its pathophysiological role in cardiovascular disease are much less understood. Especially, the role of mitochondrial oxidative stress in the pathogenesis of AAA is not clear. In angiotensin II-induced aortic aneurysm model, mitochondrial ROS may mediate inflammasome activation in macrophage during the initiation of AAA formation.[13]

Peroxiredoxins (Prdx) are a ubiquitous family of antioxidant enzymes that also control cytokine-induced peroxide levels which mediate signal transduction in mammalian cells.[14] All Prdxs share the same basic catalytic mechanism, in which an activesite cysteine (the peroxidatic cysteine) is oxidized to a sulfenic acid by the peroxide substrate. Mammals have six different Prdxs, with Prdxs 1, 2 and 6 located in the cytosol, Prdx3 in the mitochondrial matrix, Prdxs 4 in the endoplasmic reticulum and Prdx5 in mitochondria, peroxisomes and the cytosol. The potential role of Prdxs classes as novel biomarkers for AAA have been demonstrated in previous studies. Prdx1 was suggested as a biomarker for AAA [15], and Prdx2 expression was increased in ruptured abdominal aortic aneurysms compared with nonruptured abdominal aortic aneurysms.[16] However, the function of human Prdxs in the pathogenesis of AAA is still limited. Furthermore, mitochondria are major source of cellular oxidative stress, and this oxidant is implicated in the damage associated with aging and a number of pathologies. In mammals, Prdxs 3 and 5 are targeted to the mitochondrial matrix. Since Prdx3 is a mitochondrial antioxidant and the target for up to 90% of hydrogen peroxide

generated in the matrix[17], our study focused on the role of endogenous Prdx3 linking mitochondrial oxidative stress and regulation of AAA.

The purpose of the study is to investigate the role of Prdx 3 in the smooth muscle cells on the formation of AAA in 24-week-old mice model induced by angiotensin-II infusion. Furthermore, predictive role of noninvasive sonography with vascular strain method was also assessed to detect early change of AAA formation in the study.

II. MATERIALS AND METHODS

1. Experimental animal

A. Genetic background and breeding

Prdx3$^{flox/flox}$ C57BL/6J mice were provided from Prof. Sue Goo Rhee in Yonsei University. In order to produce *Prdx3*-knockout in vascular smooth muscle cells in mice, *Prdx3*$^{flox/flox}$ *SM22-Cre* model was generated by crossbreeding between *Prdx3*$^{flox/flox}$ mice and *SM22-Cre* mice. *SM22-Cre* mice (Jackson Laboratories, Bar harbor, ME, USA) have a conditional allele of a *cre* recombinase allele regulated by the smooth muscle protein-22 (sm22) promoter. *Prdx3*$^{flox/flox}$ mice were assigned as controls and *Prdx3*$^{flox/flox}$ *SM22-Cre* mice were experimental model. Female mice were used for the experiments. Control and experimental mice were fed a standard show diet for 24 weeks before implantation of osmotic pump for AAA formation. All mice were cared in accordance with the guideline of International Animal Care and Use Committee of Ewha Womans University.

B. Abdominal aortic aneurysm model

At 24 weeks, continuous infusion of angiotensin-II was started for induction of AAA by osmotic pump. Alzet mini-osmotic pump (model 2004, 0000298) from Durect Corporation (Cupertino, CA, USA) was filled with 1,200 ng/kg/min of Angiotensin II (A9525, Sigma-Aldrich, St. Louis, MO, USA). Angiotensin-II osmotic pump will be implanted as usual manner.[18] Surgical procedure for implantation of the osmotic pump was performed under anesthesia with intraperitoneal injection of ketamine (112 mg/kg) and

xylazine (11.6 mg/kg) mixture in saline. The osmotic pump was implanted subcutaneously through incision at upper back. Effect of continuous infusion of angiotensin-II was identified by serial measurement of blood pressure after implantation of the osmotic pump. After adaptation period for two weeks, stabilized measurement of blood pressure was feasible in all mice models. Blood pressure was measured every week by tail cuff with CODA system (Kent Scientific Corporation, Torrington, CT, USA). Control and experimental mice were fed a standard show diet during the experimental period and breed under same circumstances as before.

2. Assessment of abdominal aortic aneurysm

A. Ultrasound imaging

Temporal changes in aortic dimension, vascular strain, and mechanical properties were assessed by ultrasonography with Vevo 2100 system (FUJIFILM VisualSonics, Ontario, Canada). Mice were anesthetized by inhalation of 1.5-2% isoflurane with oxygen and placed on heating pad throughout the procedure of ultrasonographic imaging. Concentration and amount of inhalation gas was adjusted to keep murine heart rate ranged from 400 to 500 bpm, which is considered to indicate appropriate degree of anesthesia. Ultrasonographic probe was placed on murine abdomen after complete removal of hair. Two-dimensional mode (B-mode) was used for acquisition of trans-axial images and cine clips of abdominal aorta at the levels of inter-renal, paravisceral, and supraceliac segments. At each segment of abdominal aorta, systolic and diastolic diameters were measured. M-mode

image was also acquired to illustrate changes in aortic diameter through a pulsation cycle. Long axis images with maximally elongated plane of abdominal aorta was also captured at B-mode for measuring aortic area from inter-renal segment to segment just below diaphragm. Ultrasonographic evaluation was serially performed on day 0, 3, 7, 14, 21 and 28 after angiotensin-II infusion. Schematic study flow was illustrated in Figure 1.

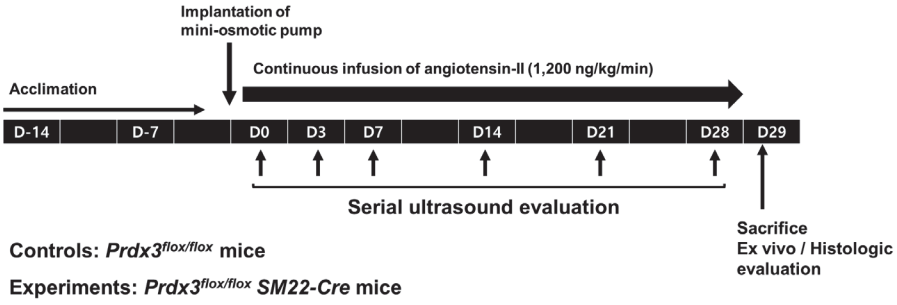

Figure 1. Schematic study flow

B. Ex vivo imaging

At 4 weeks of experimental period, mice were euthanized by carbon dioxide intoxication for autopsy. Key procedures include as followings: 1) Cutting open the mouse thoracic and abdominal cavities. 2) Cutting open right atrium to perfuse with saline, and opening left ventricle to remove blood in the aorta. 3) Harvesting aorta. 4) Fixing and cleansing aorta. Aorta was perfused with 1x phosphate-buffered saline and isolated. Aortic dilation was assessed by quantitative and semi-quantitative evaluation. First, aneurysmal area of aorta was measured by capturing and tracing the area with AxioVision software (Carl Zeiss, AxioVision AC, Germany). Second, semi-quantitative

classification was used for grading for morphological severity of AAA as follows[19,20]: Type I was defied as dilated lumen in the supra-renal region of the aorta without thrombus, type II categories remodeled tissue in the supra-renal region that frequently contains thrombus, type III indicates included bulbous aortas with visible thrombus and stage, and type IV stands for multiple aneurysms containing thrombus, some overlapping in the suprarenal area of the aorta (Figure 2). Typing of AAA was performed by three observers, who were blinded to the study allocation and experienced in experiments of mice aortic model, and majority decision was accepted for the classification.

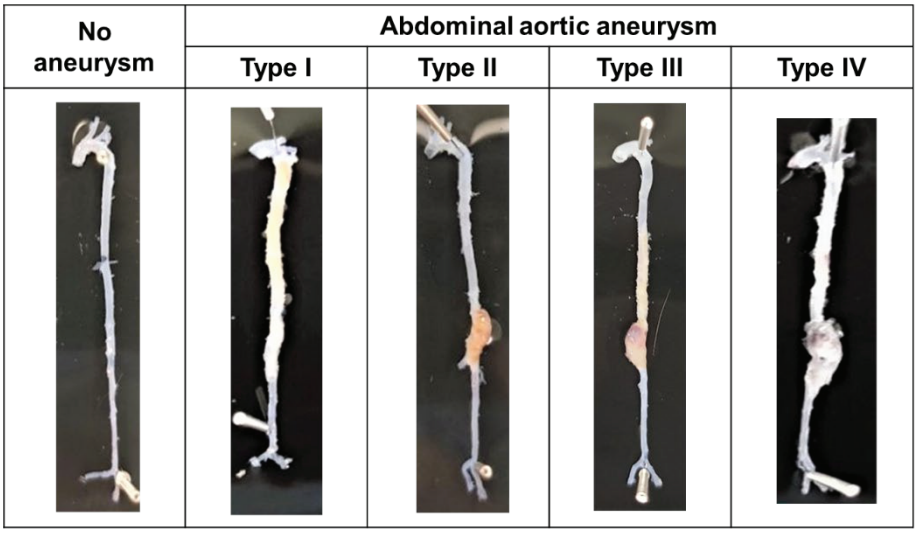

Figure 2. Representative images of each type of abdominal aortic aneurysm defined by Daugherty et al.

C. Histology for elastin degradation and calcification

Harvested abdominal aorta of mice were fixed by immersion in 10% formalin

and embedded in paraffin. Embedded block was cut into 7 μm-thick sections and attached to slides. The samples were collected onto slide at an interval of 210 μm each tissue section and stained with hematoxylin and eosin for histological tissue analysis. Russel Movat Pentachrome stain kit (KTRMP; American MasterTech Scientific, Lodi, CA, USA) was used for grading elastin degradation. Degree of elastin degradation was scored at each section of interest as follows: score 1 indicates no degradation, score 2 implies mild degradation, score 3 denotes degradation and small thrombus, and score 4 stands for big or multiple thrombus. Morphology was evaluated in at least five microphotographs for each slide by magnified images (4x and 20x) digitally captured. Calcium deposition in arterial wall was evaluated by staining with 2% Alizarin red S (A5533; Sigma-Aldrich, St. Louis, MO, USA) solution. Area of calcification which was stained by Alizarin red in the each segment of aorta was also captured and quantified by imaging process with AxioVision software (Carl Zeiss, AxioVision AC, Germany). The area of aortic calcification was also measured in at least five sections for each slide.

D. Vascular mechanics by ultrasound imaging

Vascular mechanics were measured and calculated based on trans-axial B-mode images and cine clips for detection of peak systolic and diastolic phase of aortic pulsation at each target segments. Radial wall velocity (RWV), circumferential strain (CS), and fractional area change (FAC) were measured by Vevo Strain software system (FUJIFILM VisualSonics, Ontario, Canada). RWV was calculated by difference between systolic (minimal) and diastolic

(maximal) aortic diameter during a pulsation cycle divided by time for the time between the phases captured by M-mode image. Under assumption of homogenous strain of vascular wall during a cardiac cycle, CS was calculated by the equation as previously described using the following Equation.

$$\text{Equation: CS} = 0.5 \left[\left(\frac{D_{sys}}{D_{dia}}\right)^2 - 1\right]$$

FAC was measured by percentage changes between diastolic (maximal) and systolic (minimal) aortic area. Border of outer vascular wall was manually traced on the frame of peak diastolic (maximally dilated) aorta, and the boundary line automatically traced the vascular area along cyclic pulsation by processing B-mode cine clips. The analyses of the study were performed with mean values, which were calculated by 3 values of consecutive pulsation cycles.

3. Statistical analysis

Continuous variables were expressed as mean ± S.E.M. For comparison of repeated observations including blood pressure and ultrasound-derived variables, one-way repeated ANOVA was used for comparing two groups. Bonferroni correction was adopted for post-hoc test of comparison between the time points. Considering small numbers and non-linearity, Mann-Whitney U test was performed for comparison between the groups. Phenotyping grade of AAA was considered as ordinal variable and its comparison between the groups was performed by Cochran-Armitage trend test. Relative elastin degradation score was averaged and compared by Student's T-test. To test predictability of early changes in dimensional and mechanical parameters acquired by ultrasound

imaging and postprocessing, prediction model was adopted by using Random Forest model, which is operated by constructing decision trees for classification and prediction of individual trees.[21] Variable importance score was generated and ranked in the model by using package 'varImp' command from 'caret' package in R statistics software.[22] For analysis of the predictive value of each model including dimensional parameters or including mechanical parameters, area under the curve was calculated. P-value <0.05 was considered to be statistically significant and significance was indicated by asterisk (* < 0.05, ** < 0.01, *** < 0.001).

III. RESULTS

1. Response to blood pressure by infusion of angiotensin-II

Angiotensin-II was infused by mini-osmotic pump, which is designed to maintain consistent administration of drug subcutaneously in mice model. Response to blood pressure is considered as an indirect parameter to verify continuous effect of drug throughout the study period. Baseline blood pressure was stabilized after acclimation period for sufficient adaptation of measuring blood pressure for 2 weeks in the models. As infusion of angiotensin-II was started via implanted osmotic pump, blood pressure was gradually elevated in both control and experimental mice without significant difference. Elevation of blood pressure was consistently shown during the study period with angiotensin-II infusion as intended (Figure 3).

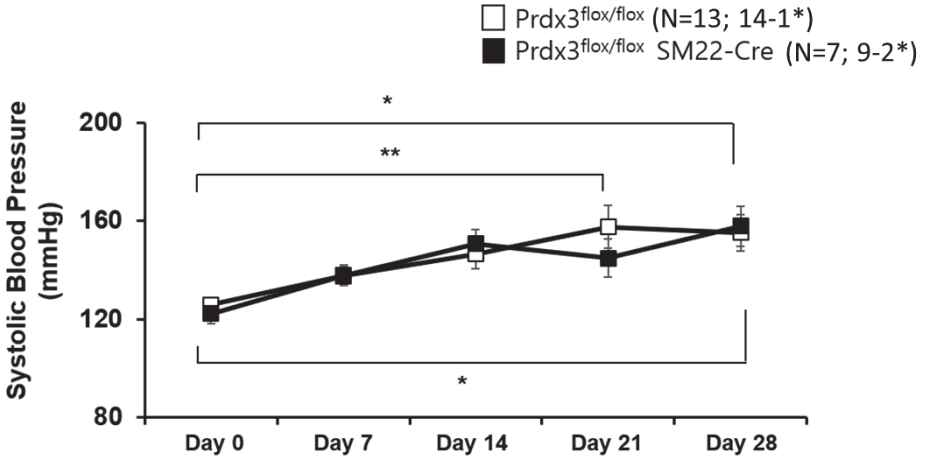

Figure 3. Serial change in systolic blood pressure during study period in the mice models. Blood pressure was steadily elevated until 4 weeks without difference between control and experimental models.

2. **Serial changes in aortic dimension and vascular mechanics**

A. **Effect of *Prdx3* knockout in vascular smooth muscle cells**

AAA was induced in 5 (36%) *Prdx3*$^{flox/flox}$ mice and 5 (55%) *Prdx3*$^{flox/flox}$ *SM22-Cre* mice during 4-week study period. In control mice with AAA, aneurysmal change of aorta was identified within 2 weeks after angiotensin-II infusion (2 mice at 1 week and 3 mice at 2 weeks). However, aneurysmal change was found from 2 to 4 weeks in experimental mice. Baseline aortic dimensions were measured before implantation of osmotic pump. Diastolic aortic diameters in *Prdx3*$^{flox/flox}$ mice were 8.3, 10.9, and 11.3 mm at inter-renal, paravisceral, and supraceliac segments, respectively. Baseline aortic diameter were similar between the control and experimental models. Baseline vascular mechanics including RWV, CS, and FAC were measured at each segment of aorta. There were no significant differences in RWV, CS, and FAC between the models (Table).

Table. Ultrasound-based measurement regarding diameter and mechanical parameters of abdominal aorta in *Prdx3*$^{flox/flox}$ and *Prdx3*$^{flox/flox}$ *SM22-Cre* mice at baseline

Parameters	*Prdx3*$^{flox/flox}$ (N=14)	*Prdx3*$^{flox/flox}$ *SM22-Cre* (N=9)
Mean aortic diameter, mm		
Inter-renal	8.3 ± 0.6	7.9 ± 0.5
Paravisceral	10.8 ± 0.8	10.3 ± 0.7
Supraceliac	11.5 ± 1.3	10.8± 0.6
RWV, mm/s		
Inter-renal	4.7 ± 1.7	4.0 ± 1.3
Paravisceral	7.7 ± 2.8	6.5 ± 1.0
Supraceliac	6.5 ± 1.8	6.4 ± 1.1
CS, %		
Inter-renal	-10.6 ± 3.6	-10.6 ± 5.4
Paravisceral	-11.4 ± 3.8	-12.1 ± 4.7
Supraceliac	-10.9 ± 3.7	-10.6 ± 4.3
FAC, %		
Inter-renal	22.1 ± 6.7	22.0 ± 6.2
Paravisceral	22.1 ± 4.5	25.3 ± 5.7
Supraceliac	17.8 ± 4.5	18.6 ± 2.7

Mean aortic diameter was slightly increased during study period at paravisceral and supraceliac segments. However, there was no increase in aortic diameter among mice which did not occur AAA formation during study period. Increase in mean aortic diameter were reflected by AAA formation. However, aortic diameter or its temporal changes was not influenced by conditional knockout of *Prdx3* vascular smooth muscle cells (Figure 4).

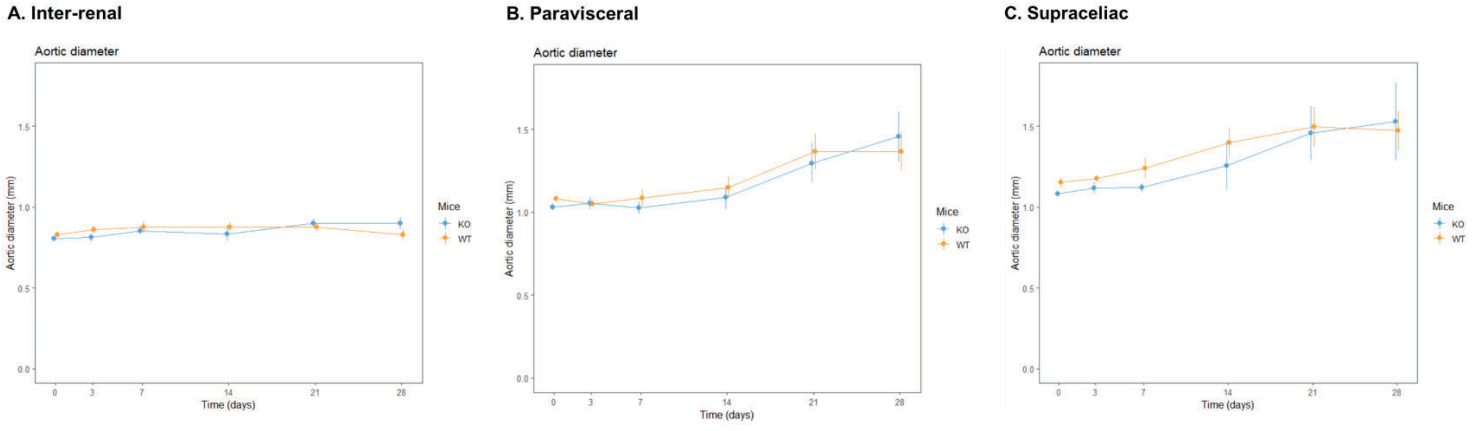

Figure 4. Serial change in mean aortic diameter in *Prdx3*$^{flox/flox}$ and *Prdx3*$^{flox/flox}$ *SM22-Cre* mice.

Aortic area was also gradually increased during study period. Aortic area tended to be greater in *Prdx3*$^{flox/flox}$ *SM22-Cre* mice since 3 weeks of angiotensin-II infusion; however, there was no significant difference in aortic area between two groups.

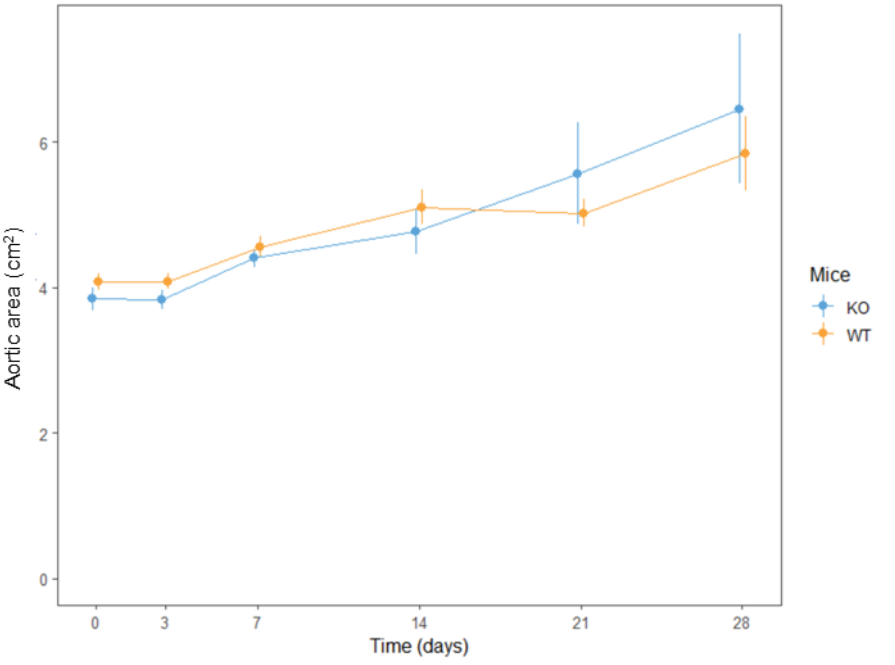

Figure 5. Serial change in aortic area in *Prdx3*$^{flox/flox}$ and *Prdx3*$^{flox/flox}$ *SM22-Cre* mice.

Vascular mechanics including were serially measured at each segment of aorta. RWV seemed to be slightly decreased over time in both models; however, there was no significant interval change in RWV at each segment of abdominal aorta and no differences in RWV between two models (Figure 6). As standard error and temporal variation of CS is wide, there was no association between *Prdx3* knockout in vascular smooth muscle cells and CS (Figure 7). Figure 8 illustrated that FAC showed significantly decreased during study period. Such temporal change was more profound at paravisceral and supraceliac segment compared with those at inter-renal segment. However, conditional knockout of *Prdx3* did not impact on the pattern of changes in FAC during the period.

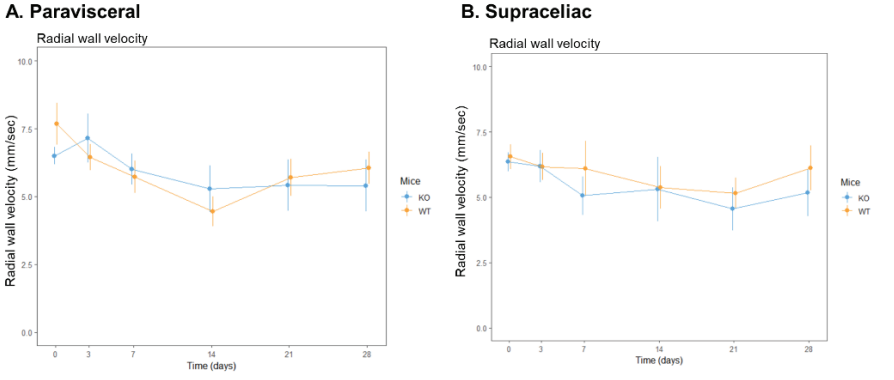

Figure 6. Serial change in radial wall velocity in *Prdx3*$^{flox/flox}$ and *Prdx3*$^{flox/flox}$ *SM22-Cre* mice.

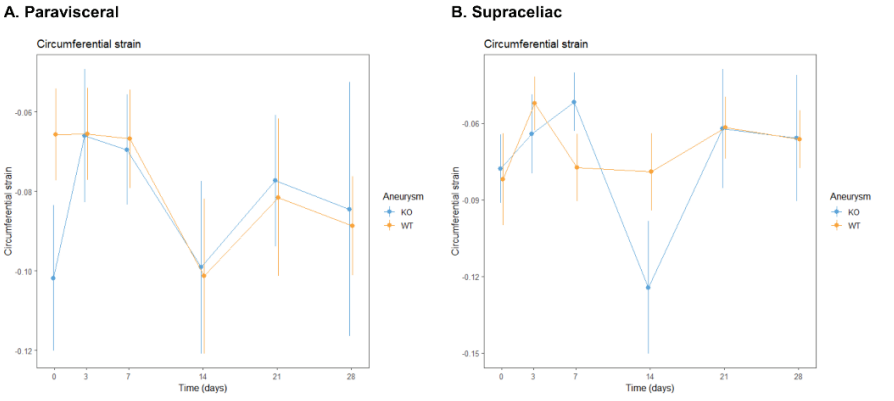

Figure 7. Serial change in circumferential strain measured in *Prdx3*$^{flox/flox}$ and *Prdx3*$^{flox/flox}$ *SM22-Cre* mice.

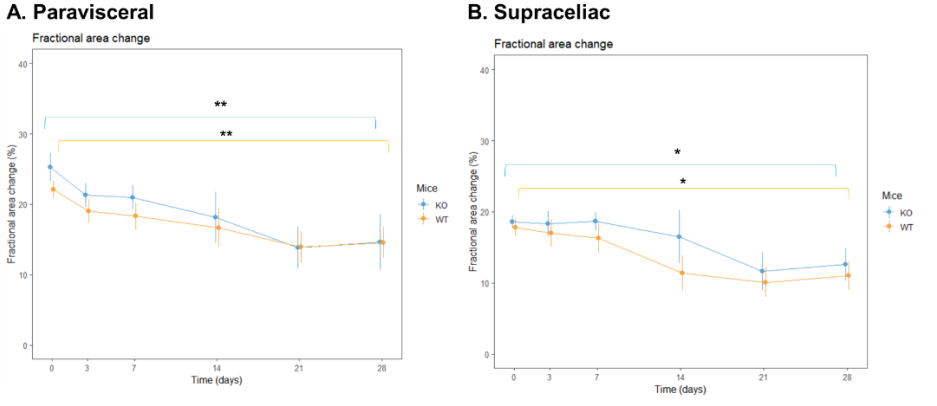

Figure 8. Serial change in fractional area change of abdominal aorta in *Prdx3*$^{flox/flox}$ and *Prdx3*$^{flox/flox}$ *SM22-Cre* mice.

B. **Abdominal aortic aneurysm and vascular mechanics**

Aortic dimensions including diameter and area were increased significantly in mice with AAA formation compared with non-diseased mice (Figures 9, 10). Aortic diameter at paravisceral and supraceliac segments and aortic diameter were rapidly increased after 2 weeks since angiotensin-II infusion in mice models occurring AAA.

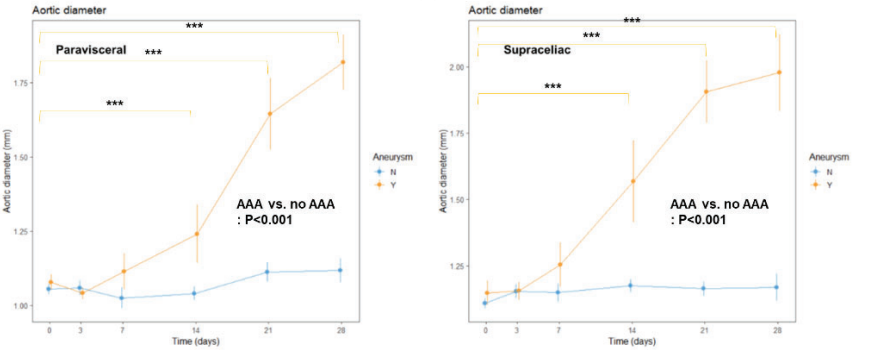

Figure 9. Serial change in aortic diameter at paravisceral and supraceliac segments according to occurrence of abdominal aortic aneurysm

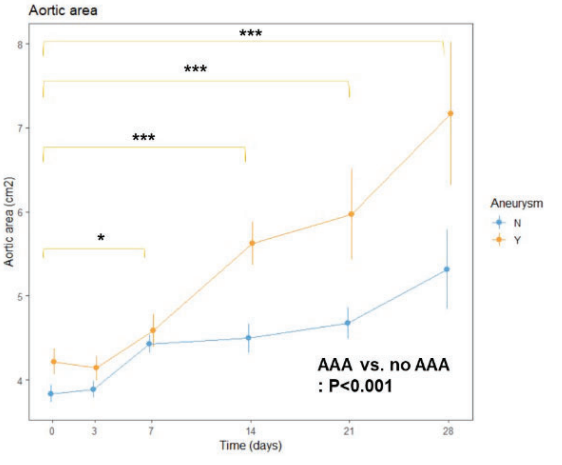

Figure 10. Serial change in aortic area according to aortic aneurysm

While RWV was maintained in mice without AAA, it was gradually decreased from very early period at both paravisceral and supraceliac segment. Change in RWV during first 7 days was significant at paravisceral segment (Figure 11). However, there was no significant association between AAA and CS (Figure 12).

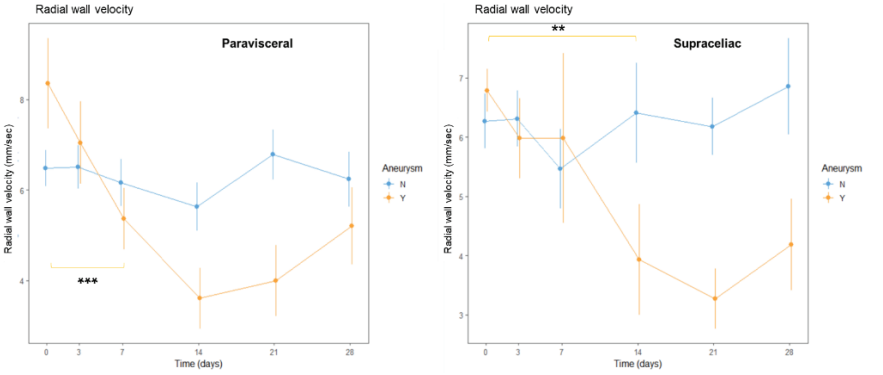

Figure 11. Serial change in radial wall velocity according to aortic aneurysm

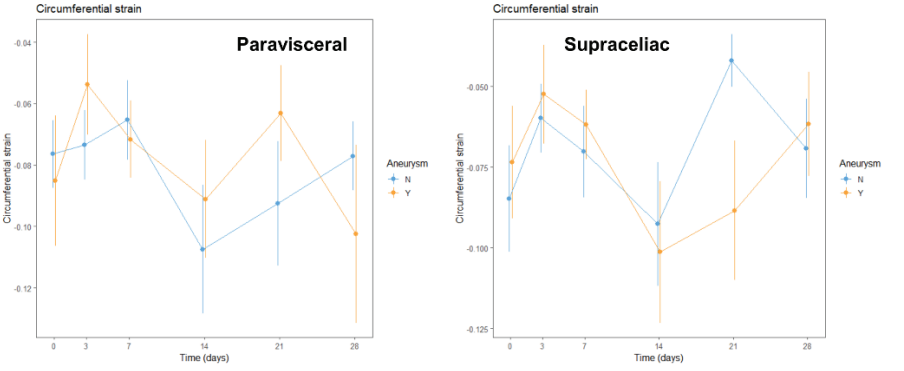

Figure 12. Serial change in circumferential strain according to aortic aneurysm

Patterns of changes in FAC is similar to those in RWV. FAC at paravisceral segment was decreased just after angiotensin-II infusion in mice generating AAA while there was no significant change during 4 weeks in mice without AAA. Statistical difference in FAC at paravisceral segment presented at 7 days (Figure 13). Vascular mechanics except CS was changed at very early period after angiotensin-II infusion especially at the level of paravisceral segment.

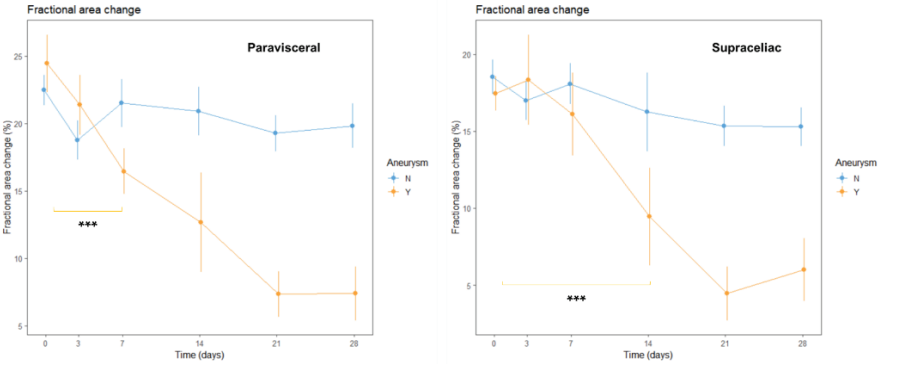

Figure 13. Serial change in fractional area change according to aortic aneurysm

3. **Ex vivo assessment: *Prdx3* knockout and severity of AAA**

Digital image of aorta isolated after 28 days of infusion of angiotensin-II was acquired by dedicated imaging software and used for grading phenotype of AAA and measuring aortic aneurysmal area. Among AAA occurred in 5 (36%) *Prdx3*$^{flox/flox}$ and 5 (55%) *Prdx3*$^{flox/flox}$ *SM22-Cre* mice, more severe phenotype of AAA was frequent in *Prdx3*$^{flox/flox}$ *SM22-Cre* mice. Of 5 *Prdx3*$^{flox/flox}$ *SM22-Cre* mice having AAA, 4 mice were classified to generate type 4 AAA, whereas type 4 AAA was not found in *Prdx3*$^{flox/flox}$ mice. Although there was no significant difference in the incidence of AAA between two mice models, there was a trend to have more aggravated form of AAA in *Prdx3*$^{flox/flox}$ *SM22-Cre* mice compared with *Prdx3*$^{flox/flox}$ mice (P=0.10 for trend, Figure 14).

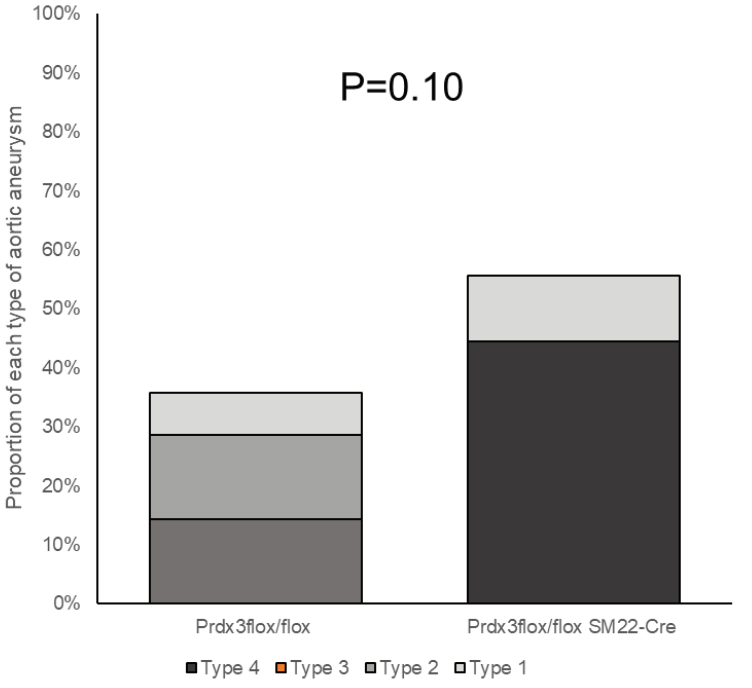

Figure 14. Incidence of each type of angiotensin-II-induced aortic aneurysm in *Prdx3*$^{flox/flox}$ and *Prdx3*$^{flox/flox}$ *SM22-Cre* mice at 28 days. AAA denotes abdominal aortic aneurysm.

Aneurysmal area was also measured and compared between *Prdx3*$^{flox/flox}$ and *Prdx3*$^{flox/flox}$ *SM22-Cre* mice. Even excluding 1 case of ruptured AAA, mean aneurysmal area of *Prdx3*$^{flox/flox}$ *SM22-Cre* mice was significantly greater (19.5%) than that of *Prdx3*$^{flox/flox}$ mice (7.7%, P<0.001, Figure 15).

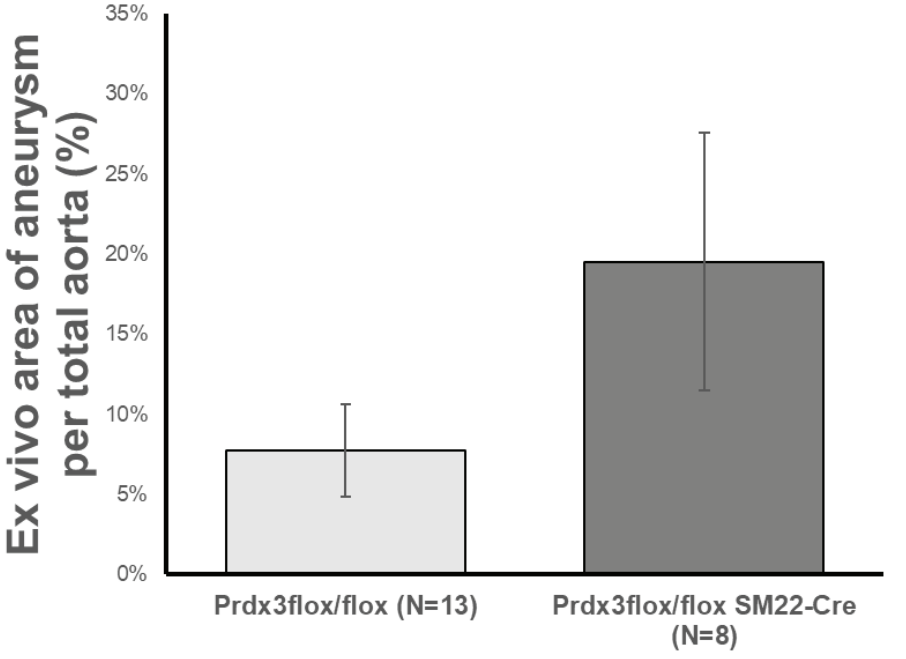

Figure 15. Ex vivo analysis of aneurysmal area in *Prdx3*$^{flox/flox}$ and *Prdx3*$^{flox/flox}$ *SM22-Cre* mice at 28 days.

4. **Histologic evaluation**

Because 1 case of AAA was ruptured before harvest aorta in *Prdx3*$^{flox/flox}$ *SM22-Cre* mice, histologic analysis was performed in AAA segments of 5 *Prdx3*$^{flox/flox}$ and 4 *Prdx3*$^{flox/flox}$ *SM22-Cre* mice.

A. Elastin degradation

Grading of elastin degradation was performed as a semi-quantitative manner at each slides of interest in segment of AAA. Nevertheless, it is found that mean relative elastin degradation scores were 2.4 and 3.6 in *Prdx3*$^{flox/flox}$ and *Prdx3*$^{flox/flox}$ *SM22-Cre* mice, respectively (P=0.04). The findings indicate that greater burden of elastin breakage and thrombus was more frequent in AAA occurred in *Prdx3*$^{flox/flox}$ *SM22-Cre* mice than those in *Prdx3*$^{flox/flox}$ mice (Figure 16).

B. Vascular calcification

Alizarin red S stained area was used for quantification of calcific burden of AAA. Figure 17 shows different patterns of aortic calcification in *Prdx3*$^{flox/flox}$ and *Prdx3*$^{flox/flox}$ *SM22-Cre* mice. Mean calcified area of AAA in *Prdx3*$^{flox/flox}$ *SM22-Cre* mice was significantly greater than that in *Prdx3*$^{flox/flox}$ mice (11.5% vs. 23.5%, P=0.02). The findings indicate that *Prdx3* deficiency in vascular smooth muscle cells accelerated deposition of calcification in aneurysmal area.

(A)

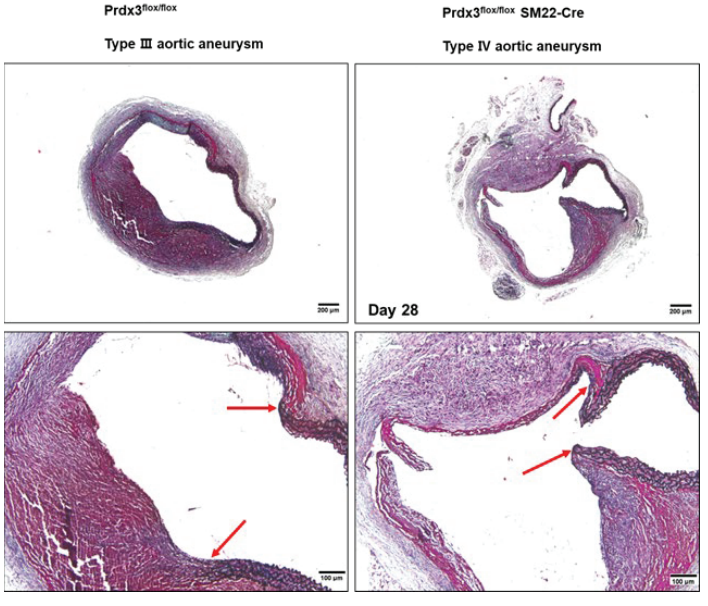

(B)

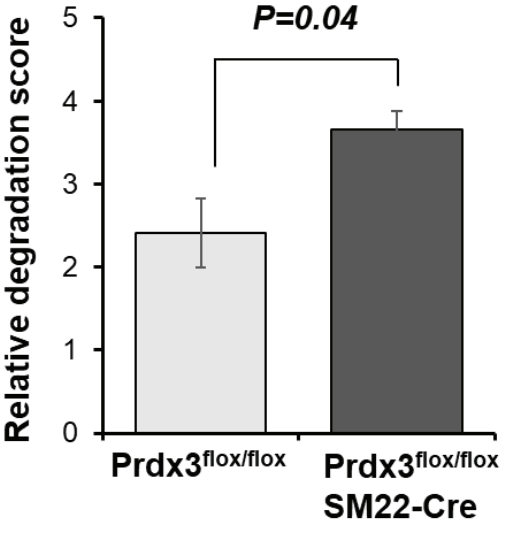

Figure 16. Patterns of elastin degradation in abdominal aortic aneurysm in *Prdx3*$^{flox/flox}$ and *Prdx3*$^{flox/flox}$ *SM22-Cre* mice at 28 days. (A) Representative aortic images for analysis of elastin degradation using Pentachrome staining. Upper and lower panels showed 4x and 20x magnification images, respectively. Arrows indicate degradation of elastin fiber. (B) Semi-quantitative comparison of elastin degradation.

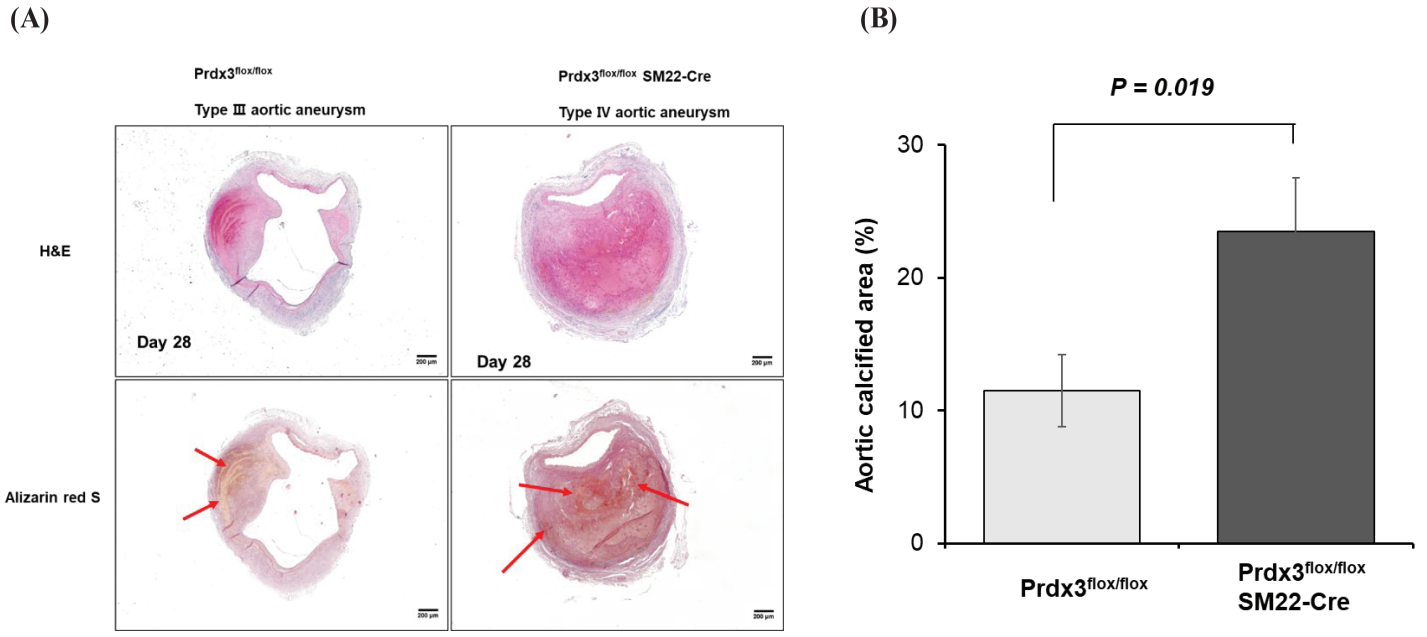

Figure 17. Analysis of degree of calcification in abdominal aortic aneurysm in *Prdx3*$^{flox/flox}$ and *Prdx3*$^{flox/flox}$ *SM22-Cre* mice at 28 days. (A) Representative aortic models for analysis of aortic calcium deposition using H&E (upper panels) and Alizarin red S stain (lower panels). Red arrows indicate calcium deposition in aortic wall. (B) Quantitative analysis of calcium deposition in terms of calcified area was chosen by stained area with Alizarin red S in aortic aneurysm.

5. **Predictive role of vascular mechanics**

In the analysis, the association between early changes in vascular mechanics and dimensional parameters and development of AAA was investigated. Interval change between at baseline and 7 days in each parameter was included in the prediction model. Random forest model including the parameters was suggested to predict AAA. Relative importance of each variable for prediction of AAA was illustrated in Figure 18. Early changes in RWV and FAC at paravisceral and supracelialc segment have greatest importance for prediction of impending AAA. However, predictive value of CS was not remarkable in the model. Early change in aortic diameter at supraceliac segment, which is most commonly involved with aneurysmal change, had greater importance than other dimensional parameters for predicting AAA. Performance of two prediction models including early changes in dimensional parameters (Model 1) and early changes in vascular mechanics (Model 2) were illustrated in Figure 19. Area under curve of Model 2 was 0.773, which was greater than that of Model 1 (0.664). These diagnostic tests imply that prediction of impending AAA would be more efficient when vascular mechanics were considered for the prediction.

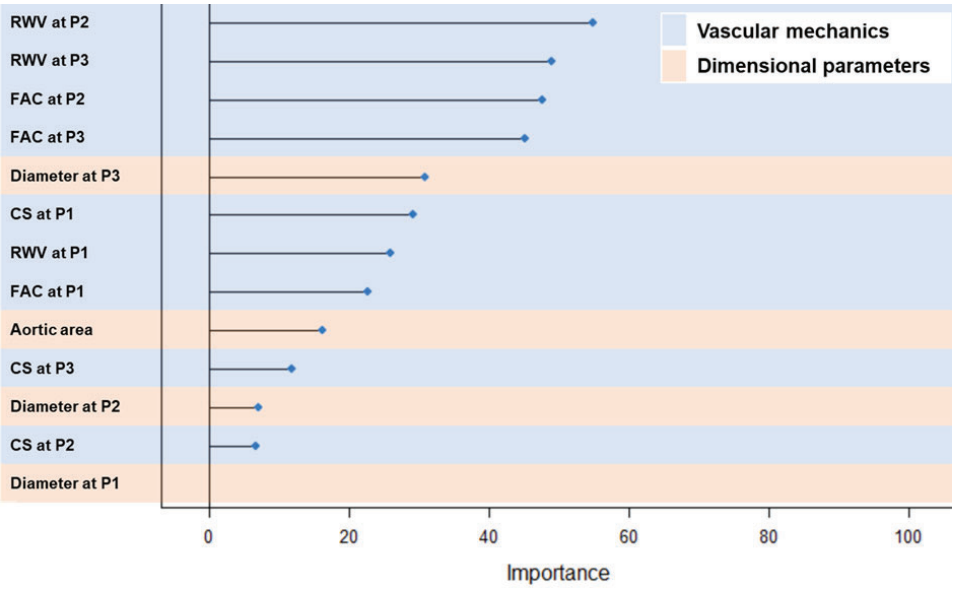

Figure 18. Relative importance of early changes in vascular mechanics and aortic dimension for predicting impending aortic aneurysm. P1, P2, and P3 indicate inter-renal, paravisceral, and supraceliac level of abdominal aorta.

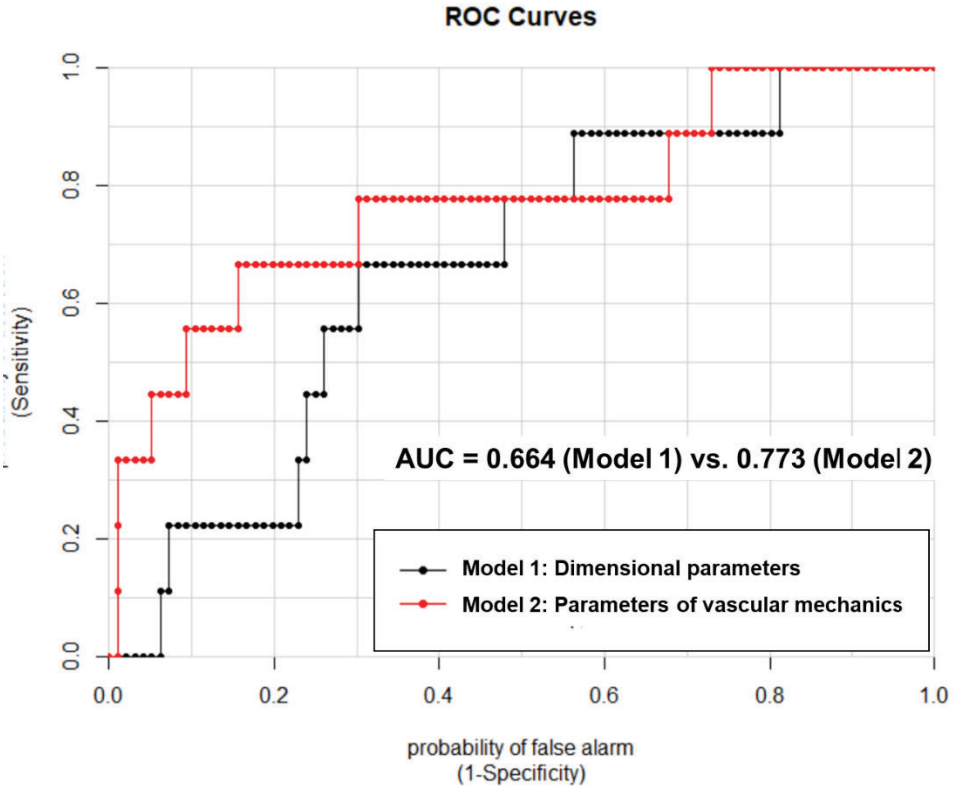

Figure 19. Predictability for impending aortic aneurysm using early changes in dimensional parameters and vascular mechanics. The area under curve (AUC) illustrates the correlation between (1-specificity) and sensitivity of the prediction model. Conventional logistic regression model was adopted for the prediction in each model including parameters of interest. Greater AUC value stands for better predictive performance.

IV. DISCUSSION

In the study, *Prdx3*$^{flox/flox}$ *SM22-Cre* mice were generated to eliminate the effect of *Prdx3* in vascular smooth muscle cells on the development of AAA. It is reasonable that conditional knockout of *Prdx3* in vascular smooth muscle cells may increase mitochondrial oxidative stress because of lacking effective elimination of oxidative stress in the vessels. The findings of present study support the potential risk of increasing oxidative stress on AAA formation. Although the incidence of AAA was not significantly influenced by *Prdx3* deficiency, it was more aggravated and severe if occurred in mice with *Prdx3* deficiency in vascular smooth muscle cells. The findings are concordant with histological analysis that conditional *Prdx3* deficiency in vascular smooth muscle cells was associated with facilitated degradation of elastin and deposition of calcium at diseased vessels. Because most cases of AAA abruptly occurred, morphological or anatomical changes such as gradual dilatation of aortic dimension was not predictive for incidence of AAA. Instead, vascular mechanics such as RWV and FAC seemed to be more useful for prediction of AAA in the mice models.

Previous studies have pointed out the close interaction between oxidative stress and many diseases or aging processes. Oxidative stress causes cellular dysfunctions and degeneration, that oxidative stress can provide a link between most known mechanisms of AAA. However, its value as the crucial key indicator or relevant mechanisms are still limited. Overproduction of ROS may subsequently induce inflammation, matrix metalloproteinase activity, smooth muscle cell apoptosis or changes in collagen properties.[23,24] Oxidative stress is

invariably increased in, and contributes importantly to, the pathophysiology of inflammation. Oxidative stress can be defined as tissue damage occurring secondary to increased production and/or decreased destruction of ROS. Thus, the balance between production and destruction of ROS depends not only on the activity of ROS-generating systems.[25]

A mitochondrial antioxidant protein, Prdx3 has been known to control tissue remodeling, extracellular matrix degradation and pathogenesis of malignancy.[26,27] In cardiovascular field, a protective role of Prdx3 was suggested that its overexpression prevents left ventricular remodeling and heart failure after myocardial infarction.[28] However, overexpression of Prdx3 was also shown to be associated with ventricular dysfunction and adverse cardiac remodeling in patients with dilated cardiomyopathy.[29] In recent study accompanied with this research, Lee demonstrated a protective role of Prdx3 on formation of AAA in young mice models (8-10 weeks old).[30] The study showed lack of Prdx3 in vascular smooth muscle cells was significantly associated with increased incidence of AAA in young mice. The present study supports the role of Prdx3 on aggravation of AAA in mature mice models. However, tremendous area of the knowledge regarding mitochondrial oxidation and its scavenging protein for the pathogenesis and protection of cardiovascular disease is unexplored yet.

Most *in vivo* assessment of AAA was used by conventional method of sonography, which can evaluate the morphology, size, and basic hemodynamics of abdominal aorta. However, the diagnostic value of sonography in the early phase of AAA formation is not well evaluated. Many clinical and experimental trials support the role of strain imaging method to diagnose the early change of

diseased status or to predict the disease progression. Vascular stiffness has been known as important cardiovascular risk factor beyond traditional clinical risk factors.[31,32] Ultrasonographic vascular mechanics have been studied for diagnosis of early pathogenesis of varying cardiovascular disease in human researches.[33] Vascular stiffness implies resistance to vascular deformation and a reduced capacity for arterial expansion and recoil. Clinical studies demonstrated impaired vascular mechanics in patients with AAA. In three-dimensional ultrasound speckle tracking analysis of human aorta, reduced strain and more pronounced temporal dyssynchrony was shown to be associated with AAA.[34] Clinical studies have been also suggested that vascular mechanics of carotid artery would be useful as a more sensitive method for assessment of vascular stiffness compared with conventional ultrasonographic evaluation. Previous clinical researches demonstrated that impaired vascular mechanics is independently associated with hypertension, severity of coronary atherosclerosis, and increased cardiovascular risk.[35-37] Furthermore, the other previous study reported that reduced aortic strain and distensibility is a sensitive and specific marker of vascular aging in young age adult.[38] Such findings suggest that novel aortic mechanics may have a prognostic value; however, it is still limited that prognostic value of vascular strain or other metrics reflecting vascular function is uncertain. As it requires large amount of resources including long-term longitudinal studies including large number of participants to verify the prognostic role of such sensitive markers, it should examine the hypothesis of prognostic role of vascular mechanics on degenerative vascular disease. In the study, early changes in vascular circumferential strain occurred in the mice which developed AAA by

angiotensin-II infusion. In clinical study, impaired vascular strain is obviously seen in both thoracic and abdominal aortic aneurysm.[39] The findings of previous studies imply that diseased and dilated segment of aorta lose vasomotor activity not only in the diseased segment but also in the adjacent segment.[39] It is possible that such mechanical impairment may be prescient for further expansion or aggravation of AAA. Similar to the clinical research, our induced AAA model had significantly impaired vascular mechanical profiles including radial wall velocity, circumferential strain, and fractional area change compared with the subjects without AAA formation. Importantly, early detection of changes in vascular mechanics may play a prognostic role on the degenerative vascular disease as we demonstrated in the study. Dimensional change was not predictable before occurrence of AAA. It is notable that aortic dilation and formation of AAA was not gradually induced in the experimental models. As early progress and formation of AAA is hardly known, it may be reasonable that impaired vascular integrity and function, which would be only measurable by very sensitive methods, may be linked to rapid progression of aneurysmal change. Literatures and the findings of the study also supports that vascular mechanics may be useful to assess impairment of subclinical vascular integrity and function and to predict vascular dilation and aneurysmal formation. Further studies will be needed to establish the prognostic value of vascular mechanics with more detailed strain indices and its association at each stage. It should be concerned that vascular mechanics assessed by ultrasound sonography in the mice model may not be identically applied to the other experimental model. Because it has not been known about the reference range of vascular mechanical metrics in the mice

model, serial changes and comparisons between the comparable groups were only measured and assessed. As ultrasound is known to be user-dependent, reproducibility of the measurements may differ according to the experimental models. Vascular measurements may also be influenced by sympathetic activity and anesthesia of the mice model and would affect the consistency of measurements. Further studies may be extended to the other models having different genetic background, age, and atherogenic conditions. As vascular mechanics assessed by three-dimensional ultrasound and magnetic resonance imaging is feasible in clinical studies, novel diagnostic tools and metrics may be also promising for prediction of degenerative vascular disease.

V. CONCLUSION

Deficiency of Prdx3 in vascular smooth muscle cells impacted on aggravation of angiotensin-II-induced AAA including elastin degradation and calcium deposition in 24-week mice models. Early changes in vascular mechanics including RWV and FAC played a predictive role for impending AAA while changes in aortic dimension did not impact on the incidence of AAA. Novel diagnostic methods to detect sensitive changes in vascular mechanics assuring feasibility and reproducibility may be promising for risk stratification and early detection of degenerative vascular disease.

REFERENCES

1. Weintraub NL. Understanding Abdominal Aortic Aneurysm. N Engl J Med 2009;361:1114-6.
2. Lubrano V, Balzan S. Enzymatic antioxidant system in vascular inflammation and coronary artery disease. World J Exp Med 2015;5:218-24.
3. Miller FJ, Jr., Sharp WJ, Fang X, Oberley LW, Oberley TD, Weintraub NL. Oxidative stress in human abdominal aortic aneurysms: a potential mediator of aneurysmal remodeling. Arterioscler Thromb Vasc Biol 2002;22:560-5.
4. Cafueri G, Parodi F, Pistorio A, Bertolotto M, Ventura F, Gambini C, et al. Endothelial and smooth muscle cells from abdominal aortic aneurysm have increased oxidative stress and telomere attrition. PLoS One 2012;7:e35312.
5. Pincemail J, Defraigne JO, Cheramy-Bien JP, Dardenne N, Donneau AF, Albert A, et al. On the potential increase of the oxidative stress status in patients with abdominal aortic aneurysm. Redox Rep 2012;17:139-44.
6. Papalambros E, Sigala F, Georgopoulos S, Paraskevas KI, Andreadou I, Menenakos X, et al. Malondialdehyde as an indicator of oxidative stress during abdominal aortic aneurysm repair. Angiology 2007;58:477-82.
7. Guzik B, Sagan A, Ludew D, Mrowiecki W, Chwała M, Bujak-Gizycka B, et al. Mechanisms of oxidative stress in human aortic aneurysms — Association with clinical risk factors for atherosclerosis and disease severity. Int J Cardiol 2013;168:2389-96.

8. Burillo E, Tarin C, Torres-Fonseca M-M, Fernandez-García C-E, Martinez-Pinna R, Martinez-Lopez D, et al. Paraoxonase-1 overexpression prevents experimental abdominal aortic aneurysm progression. Clin Sci (Lond) 2016;130:1027-38.

9. Kigawa Y, Miyazaki T, Lei XF, Kim-Kaneyama JR, Miyazaki A. Functional Heterogeneity of Nadph Oxidases in Atherosclerotic and Aneurysmal Diseases. J Atheroscler Thromb 2017;24:1-13.

10. Guzik B, Sagan A, Ludew D, Mrowiecki W, Chwala M, Bujak-Gizycka B, et al. Mechanisms of oxidative stress in human aortic aneurysms--association with clinical risk factors for atherosclerosis and disease severity. Int J Cardiol 2013;168:2389-96.

11. Dikalov S. Cross talk between mitochondria and NADPH oxidases. Free Radic Biol Med 2011;51:1289-301.

12. Dikalov SI, Ungvari Z. Role of mitochondrial oxidative stress in hypertension. Am J Physiol Heart Circ Physiol 2013;305:H1417-H27.

13. Usui F, Shirasuna K, Kimura H, Tatsumi K, Kawashima A, Karasawa T, et al. Inflammasome activation by mitochondrial oxidative stress in macrophages leads to the development of angiotensin II-induced aortic aneurysm. Arterioscler Thromb Vasc Biol 2015;35:127-36.

14. Wood ZA, Schroder E, Robin Harris J, Poole LB. Structure, mechanism and regulation of peroxiredoxins. Trends Biochem Sci 2003;28:32-40.

15. Martinez-Pinna R, Ramos-Mozo P, Madrigal-Matute J, Blanco-Colio LM, Lopez JA, Calvo E, et al. Identification of Peroxiredoxin-1 as a Novel Biomarker of Abdominal Aortic Aneurysm. Arterioscler Thromb

Vasc Biol 2011;31:935-43.

16. Urbonavicius S, Lindholt JS, Vorum H, Urbonaviciene G, Henneberg EW, Honore B. Proteomic identification of differentially expressed proteins in aortic wall of patients with ruptured and nonruptured abdominal aortic aneurysms. J Vasc Surg 2009;49:455-63.
17. Cox AG, Winterbourn CC, Hampton MB. Mitochondrial peroxiredoxin involvement in antioxidant defence and redox signalling. Biochem J 2009;425:313-25.
18. Lu H, Howatt DA, Balakrishnan A, Moorleghen JJ, Rateri DL, Cassis LA, et al. Subcutaneous Angiotensin II Infusion using Osmotic Pumps Induces Aortic Aneurysms in Mice. J Vis Exp 2015.
19. Daugherty A, Manning MW, Cassis LA. Antagonism of AT2 receptors augments angiotensin II-induced abdominal aortic aneurysms and atherosclerosis. Br J Pharmacol 2001;134:865-70.
20. Hadi T, Boytard L, Silvestro M, Alebrahim D, Jacob S, Feinstein J, et al. Macrophage-derived netrin-1 promotes abdominal aortic aneurysm formation by activating MMP3 in vascular smooth muscle cells. Nat Commun 2018;9:5022.
21. Breiman L. Random Forests. Mach Learn 2001;45:5-32.
22. Kuhn M. Building predictive models in R using the caret package. J Stat Softw 2008;28:1-26.
23. Wenzel P, Kossmann S, Münzel T, Daiber A. Redox regulation of cardiovascular inflammation – Immunomodulatory function of mitochondrial and Nox-derived reactive oxygen and nitrogen species.

Free Radic Biol Med 2017;109:48-60.

24. Schramm A, Matusik P, Osmenda G, Guzik TJ. Targeting NADPH oxidases in vascular pharmacology. Vascul Pharmacol 2012;56:216-31.

25. McCormick ML, Gavrila D, Weintraub NL. Role of Oxidative Stress in the Pathogenesis of Abdominal Aortic Aneurysms. Arterioscler Thromb Vasc Biol 2007;27:461-9.

26. Liu Z, Hu Y, Liang H, Sun Z, Feng S, Deng H. Silencing PRDX3 Inhibits Growth and Promotes Invasion and Extracellular Matrix Degradation in Hepatocellular Carcinoma Cells. J Proteome Res 2016;15:1506-14.

27. Yu R, Yao J, Ren Y. A novel circRNA, circNUP98, a potential biomarker, acted as an oncogene via the miR-567/ PRDX3 axis in renal cell carcinoma. J Cell Mol Med 2020 [Online ahead of print].

28. Matsushima S, Ide T, Yamato M, Matsusaka H, Hattori F, Ikeuchi M, et al. Overexpression of mitochondrial peroxiredoxin-3 prevents left ventricular remodeling and failure after myocardial infarction in mice. Circulation 2006;113:1779-86.

29. Roselló-Lletí E, Tarazón E, Barderas MG, Ortega A, Otero M, Molina-Navarro MM, et al. Heart Mitochondrial Proteome Study Elucidates Changes in Cardiac Energy Metabolism and Antioxidant PRDX3 in Human Dilated Cardiomyopathy. PLoS One 2014;9:e112971.

30. Lee DS. Peroxiredoxin 3 Deficiency in Vascular Smooth Muscle Cells Exacerbates Abdominal Aortic Aneurysm in Mice: Ewha Womans University Graduate School; 2019.

31. O'Rourke MF. Clinical assessment of arterial stiffness. Am J Hypertens

2007;20:839.

32. Laurent S, Boutouyrie P, Cunha PG, Lacolley P, Nilsson PM. Concept of Extremes in Vascular Aging. Hypertension 2019;74:218-28.

33. Teixeira R, Vieira MJ, Gonçalves A, Cardim N, Gonçalves L. Ultrasonographic vascular mechanics to assess arterial stiffness: a review. Eur Heart J Cardiovasc Imaging 2015;17:233-46.

34. Karatolios K, Wittek A, Nwe TH, Bihari P, Shelke A, Josef D, et al. Method for aortic wall strain measurement with three-dimensional ultrasound speckle tracking and fitted finite element analysis. Ann Thorac Surg 2013;96:1664-71.

35. Kim SA, Park SM, Kim MN, Kim YH, Cho DH, Ahn CM, et al. The relationship between mechanical properties of carotid artery and coronary artery disease. Eur Heart J Cardiovasc Imaging 2012;13:568-73.

36. Park HE, Cho GY, Kim HK, Kim YJ, Sohn DW. Validation of circumferential carotid artery strain as a screening tool for subclinical atherosclerosis. J Atheroscler Thromb 2012;19:349-56.

37. Saito M, Okayama H, Inoue K, Yoshii T, Hiasa G, Sumimoto T, et al. Carotid arterial circumferential strain by two-dimensional speckle tracking: a novel parameter of arterial elasticity. Hypertens Res 2012;35:897-902.

38. Redheuil A, Yu W-C, Wu CO, Mousseaux E, de Cesare A, Yan R, et al. Reduced ascending aortic strain and distensibility: earliest manifestations of vascular aging in humans. Hypertension 2010;55:319-26.

39. de Beaufort HWL, Nauta FJH, Conti M, Cellitti E, Trentin C, Faggiano E, et al. Extensibility and Distensibility of the Thoracic Aorta in Patients with Aneurysm. Eur J Vasc Endovasc Surg 2017;53:199-205.

ABSTRACT(IN KOREAN)

쥐 모델에서 안지오텐신-II-유도 복부대동맥류 형성에 대한 혈관평활근 세포의 퍼옥시리독신 3 결핍의 영향 및 손상된 혈관 역학의 예측 효과의 연구

<지도교수 장양수>

연세대학교 대학원 의학과

김 충 기

복부대동맥류는 혈관 내에 증가된 금속단백분해효소 활성, 혈관 염증 및 산화 스트레스로 인해 유발되는 퇴행성 혈관 질환으로 알려져 있다. 퍼옥시리독신 3는 미토콘드리아에 존재하며 내부 산화 스트레스를 제거하는 데에 중요한 역할을 한다. 본 연구에서는 24주령 쥐 모델을 이용하여 실험을 진행하였으며, *Prdx3*$^{flox/flox}$ *SM22-Cre* 쥐를 생산하여, 복부대둥맥류 형성에 중요한 역할을 수행하는 혈관 평활근 세포의 퍼옥시리독신 3에 대한 선택적 넉아웃을 유도하였으며, *Prdx3*$^{flox/flox}$ 쥐가 대조군으로 사용되었다. 복부대동맥류는 피하에 주입된 미니 삼투압 펌프를 통해 지속적으로 주입되는 안지오텐신-II을 통하여 유발하였다. 연속적인 초음파 평가를 통해 복부대동맥의 형성과 진행 과정을 확인하였으며, 혈관의 모양, 치수 및 역학적

성질을 측정하였다. 14 마리의 *Prdx3*$^{flox/flox}$ *SM22-Cre* 쥐와 9마리의 대조군 중에서, 복부대동맥류는 실험군에서 5마리 (55%) 그리고 대조군에서 5마리 (36%) 발생하였다. 복부대동맥류의 발생, 초음파로 측정된 혈관의 치수 및 역학 요소들에는 큰 차이가 없었으나, 퍼옥시리독신 3은 보다 악화된 형태의 복부대동맥류와의 연관성을 보이는 경향이 있었다. 또한 대조군 쥐에서 발생한 대동맥류의 소견과 비교하여, *Prdx3*$^{flox/flox}$ *SM22-Cre* 쥐에서 발생한 대동맥류에서는 탄력소의 손상 및 석회 침착이 보다 많았다. 대동맥류가 발생하지 않은 대동맥과 비교하여, 복부대동맥류는 급격한 혈관 치수의 증가와 함께 혈관 역학의 손상이 나타났다. 추후 복부대동맥류가 발생하는 쥐에 있어서 방사벽속도 (radial wall velocity) 및 와 분획 면적 변화의 변화가 초기부터 관찰되었다. 혈관 역학의 초기 변화와 연관된 지표들을 통한 모델은 혈관 치수를 근거한 모델에 비하여 추후 복부대동맥류의 발생을 예측하는 데에 있어서 우수하였다. 높은 접근성 및 재현성을 가진 비침습적 진단검사를 통해서 추후 복부대동맥류의 위험 분류 및 진행에 대한 예측에 있어서 활용될 가능성을 기대할 수 있겠다.

핵심되는 말 : 복부대동맥류, 산화 스트레스, 퍼옥시리독신, 혈관 역학